Improving Generalization in Deepfake Detection with Face Foundation Models and Metric Learning

Stelios Mylonas
Centre for Research and Technology Hellas
Information Technologies Institute
Thessaloniki, Greece
smylonas@iti.gr

Symeon Papadopoulos
Centre for Research and Technology Hellas
Information Technologies Institute
Thessaloniki, Greece
papadop@iti.gr

Abstract

The increasing realism and accessibility of deepfakes have raised critical concerns about media authenticity and information integrity. Despite recent advances, deepfake detection models often struggle to generalize beyond their training distributions, particularly when applied to media content found in the wild. In this work, we present a robust video deepfake detection framework with strong generalization that takes advantage of the rich facial representations learned by face foundation models. Our method is built on top of FSFM, a self-supervised model trained on real face data, and is further fine-tuned using an ensemble of deepfake datasets spanning both face-swapping and face-reenactment manipulations. To enhance discriminative power, we incorporate triplet loss variants during training, guiding the model to produce more separable embeddings between real and fake samples. Additionally, we explore attribution-based supervision schemes, where deepfakes are categorized by manipulation type or source dataset, to assess their impact on generalization. Extensive experiments across diverse evaluation benchmarks demonstrate the effectiveness of our approach, especially in challenging real-world scenarios.

Keywords

Deepfake Detection, Face Foundation Models, Metric Learning, Attribution

1 Introduction

Over the last few years, the rapid advancement of generative models, particularly deep learning-based approaches, has led to the widespread circulation of highly realistic synthetic media, especially deepfakes. Deepfake videos manipulate a person's appearance or voice, enabling the creation of fabricated visual content that is difficult to distinguish from authentic footage. This technology has introduced significant risks in the modern digital society, including identity theft, fraud, political misinformation, and non-consensual content creation [8].

Over time, a variety of deepfake techniques have emerged, each manipulating different aspects of facial identity and expression. Face swapping (FS) replaces an individual's face with another while preserving natural head movements and expressions [32, 35, 42]. Face reenactment (RE) modifies facial expressions or head poses to mimic another person, allowing control over expressions, head, and even lip, movements [3, 49, 57]. Last, lip-syncing extends the manipulations to the audio-visual domain by aligning mouth movements with a given speech track, creating videos where individuals appear to say things they never did [31, 44, 55].

Given the growing accessibility of deepfake generation tools and the increasing quality of their outputs, the need for reliable detection tools has become a critical concern for professionals in the media forensics domain. In response, numerous detection techniques have been developed over the past decade, targeting a wide range of manipulations across both visual [18, 46, 48, 64] and audio-visual domains [14, 28, 43]. Despite these advances, several challenges remain unsolved. The employed supervised learning strategies usually suffer from poor generalization, as they tend to rely on manipulation-specific artifacts, leading to significant performance drops when faced with previously unseen deepfake methods [61]. This limitation becomes even more apparent in real-world scenarios, where deepfakes encountered in the wild (e.g., on social media) have undergone various post-processing operations, including compression, resolution loss, and content alterations.

Our goal in this paper is to develop a robust and generalizable model capable of handling real-world deepfake scenarios. Importantly, we aim for a general solution that can effectively address both face swapping and face reenactment manipulations. However, we also introduce certain constraints to keep the approach more practical. First, we target the most common case of vision-only manipulations, deliberately excluding the audio modality. This choice is motivated by real-world observations: many deepfake videos lack an audio track, or when present, the audio is often noisy or inaudible, which can hinder rather than help detection performance. Second, we impose a computational constraint to ensure the method remains suitable for real-time applications. Based on that, we opt for a frame-based approach, avoiding computationally intensive techniques that rely on temporal-aware representations such as 3D tensors or methods relying on face tracking, which can introduce significant computational overhead.

Building on these design choices, we propose a vision-only, frame-based detection approach tailored for real-world applicability. Our model is trained on an ensemble of training datasets, aiming to learn a broad spectrum of deepfake manipulations across diverse video capturing conditions. To improve generalization, we leverage recent advancements in facial representation learning [65], where face foundation models are developed by self-supervised training on large-scale datasets of real faces. These provide strong, transferable facial representations and have shown promise as initialization points for downstream tasks such as deepfake detection.

In our approach, we adopt one such model (FSFM [54]) as our backbone, initializing our network with its pre-trained weights before fine-tuning for our task.

To further enhance our model's discriminative capacity, we augment the training objective with an additional triplet loss, aiming to encourage more representative embeddings that can improve classification performance. Finally, we investigate the effectiveness of incorporating attribution strategies, where deepfakes are categorized by type or source during training, and compare them to standard binary classification approaches.

Our contributions are summarized as follows:

- We leverage the expressive facial representations learned by face foundation models to enhance deepfake detection performance.
- We investigate the impact of alternative triplet loss formulations and attribution strategies on detection accuracy.
- We conduct extensive experiments across various settings, including in-distribution, out-of-distribution, and in-the-wild scenarios, to rigorously evaluate the effectiveness and generalization of our approach.

2 Related work

2.1 Deepfake detection

The majority of state-of-the-art video deepfake detection methods adopt data-driven approaches that rely on advanced deep learning architectures, such as convolutional neural networks (CNNs) [29] and Transformers [52]. One of the earliest works is FaceForensics [46], where a CNN was trained on labeled datasets to distinguish between real and fake faces. Expanding on this, several newer methods [33, 41, 48, 50] replaced labeled deepfakes with pseudo-negatives that are generated dynamically during training, aiming to reduce reliance on annotated data and in that way improve generalization. For example, pseudo-fakes in [48], referred to as Self-Blended Images (SBI), are created by blending distorted versions of a single pristine image to simulate common forgery artifacts. Similarly, Latent Space Data Augmentation (LSDA) [60] and Curricular Dynamic Forgery Augmentation (CDFA) [34] augmented training with synthetic negatives to further boost performance. Other approaches explored forgery clues in the frequency domain [45, 66], while Uncovering Common Features (UCF) [62] introduced a disentanglement framework that isolates common forgery features for classification. Although some recent works have explored temporal modeling [17, 18, 58, 64] or audio-visual cues [14, 28, 43] to improve robustness, our approach focuses on a more efficient, frame-based and vision-only setup.

2.2 Facial representation learning

Self-supervised learning (SSL) has recently emerged as a powerful approach for learning transferable representations from unlabeled data. When applied to face analysis tasks, it led to the development of general-purpose facial encoders (*face foundation models*) that can serve as the backbone for various downstream applications such as facial attribute recognition, expression analysis, and landmark localization [4, 37, 56]. However, many of these early approaches primarily focus on learning global face representations, often overlooking the spatial consistency and importance of local facial regions (e.g., eyes, nose, mouth). As a result, they struggle to capture the fine-grained facial details necessary for tasks that require high sensitivity to local features.

To address this limitation, recent works have proposed frameworks that jointly model both global and local facial information. MARLIN [5] introduced a facial video masked autoencoder that leverages an external face parsing algorithm to guide its masking strategy. By identifying semantic facial regions, MARLIN applies region-guided masking during training, enabling the model to learn spatially-aware representations. FRA [15] built on the same idea by explicitly learning consistent global and local facial representations. Their approach enforces local region consistency across augmented views, encouraging the model to learn discriminative representations for key facial regions, such as eyes and nose. On the other hand, FSFM [54] specifically targeted the generalization capabilities of face representations for face security applications, including deepfake detection and face anti-spoofing. They proposed a framework that combines masked image modeling (MIM) and instance discrimination (ID) to jointly capture fine-grained local details and high-level global semantics of real faces.

2.3 Losses in deepfake detection

The standard approach in deepfake detection typically involves training models in a supervised manner using the binary softmax cross-entropy (CE) loss. While effective for maximizing classification accuracy, CE loss primarily optimizes the decision boundary separation and does not explicitly promote intra-class compactness or inter-class separability in the feature space. To address this limitation, Liu et al. [38] conducted a comprehensive evaluation of alternative loss functions, originally developed for face recognition, in the context of deepfake detection. Although no single loss consistently outperformed others across all benchmarks, the results indicated that incorporating specialized losses, such as ArcFace [9] or COCO [36], could enhance model performance on deepfake detection tasks.

In recent years, a new class of losses has emerged in the context of deep metric learning, which focuses on the separability of samples in a learned embedding space [24]. Metric learning aims to construct a representation space where semantically similar samples are mapped close together, while dissimilar ones are mapped far apart. The most commonly used loss in this domain is the triplet loss, originally introduced by Schroff et al. [47]. Despite its wide success in face recognition, triplet loss has seen very limited application in deepfake detection. Two studies incorporated triplet loss in a strategy of two-stage training [2, 30]. First, an encoder was trained with triplet loss to learn a discriminative embedding space separating real and fake samples. Secondly, a classifier was trained on top of these embeddings to perform the final classification. The incorporation of triplet loss proved quite effective, especially under limited data conditions, improving both intra-dataset and cross-dataset detection performance.

2.4 Attribution in deepfake detection

In recent years, several works have explored the attribution of synthetic media, though the majority have concentrated on the image domain. Early efforts mainly focused on identifying the source of

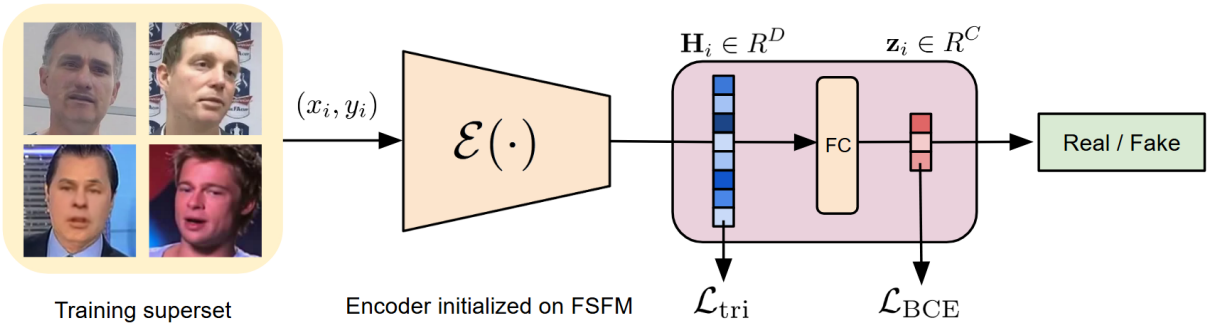

Figure 1: Flowchart of our method.

manipulation in GAN-generated images [16, 63]. However, these approaches are limited in applicability to real-world scenarios, as they primarily target very specialized synthetic content. A recent work by Khoo et al. [26] attempted to handle more advanced manipulation techniques, yet the focus still remained in the image domain.

The first work to consider attribution in the video domain was proposed by Jain et al. [21]. They trained conventional classification models, such as XceptionNet and EfficientNet, to attribute six different manipulation types, sourced from a collection of deepfake datasets. In addition to that, they explored the use of triplet loss in a two-stage training setting, very similar to the approaches followed in [2, 30]. An extension of this work [27] expanded the number of deepfake classes from six to nine and incorporated a modified ArcFace loss to enhance embedding discrimination. Similarly, Jia et al. [22] trained an attention-enhanced CNN to distinguish between five different face-swap manipulations from a custom dataset. A recent study by Baxevanakis et al. [1] evaluated the generalization capabilities of attribution models and found that, while they generally underperform compared to binary classifiers, they can benefit from higher-quality training data and the incorporation of contrastive learning, particularly in larger network architectures.

3 Proposed Method

Our proposed deepfake detection approach consists of four core components (Fig. 1): (1) training on a diverse collection of deepfake datasets to capture a wide range of manipulations and capturing conditions, (2) initializing the model with FSFM, a self-supervised face foundation model pre-trained on real facial data, (3) jointly optimizing a classification objective (cross-entropy loss) and an embedding separation objective (triplet loss), and (4) exploring attribution-based supervision strategies. The following subsections detail each of these components.

3.1 Multi-dataset training

From a machine learning perspective, video deepfake detection is typically framed as a binary classification problem, discriminating between pristine and deepfake videos. This study adopts a supervised learning approach, necessitating a labeled dataset of real and fake videos for model training. The standard practice in the literature involves training models on the FaceForensics++ (FF++) dataset [46] and then evaluating their generalization on unseen datasets. However, this choice is primarily driven, not by the intrinsic quality of FF++, but from the need for backward compatibility so as to facilitate comparison with earlier publications. FF++ is a relatively small first generation deepfake dataset that contains older manipulation techniques and is characterized by lower-quality manipulated faces and artifacts easily detectable by the human eye [51]. Consistent with this, a user study by Jiang et al. [23] assigned FF++ the lowest "realness" score among seven deepfake datasets available at that time.

Since our objective is to develop a model capable of efficiently handling real-world deepfake cases, rather than directly comparing with previous publications, we chose to train our models not solely on FF++, but on an ensemble of five different datasets: FF++ [46], Celeb-DF [33], DFDC [12], FakeAVCeleb [25] and ForgeryNet [19]. The latter four datasets are all newer than FF++ and significantly expand our training pool, offering not only more samples but also a broader spectrum of manipulation types (both FS and RE). This new hyper-set should enable the model to learn from a sufficiently large and diverse set of manipulation methods, thereby enhancing its detection capabilities.

Furthermore, another crucial point favoring multi-dataset training is the inherent limitations of individual datasets. Each dataset is typically created under specific conditions concerning both scene characteristics (e.g., camera angle, lighting, indoor/outdoor environment) and the demographic traits of participants (e.g., race, gender, age). Such limitations in diversity can negatively impact a model's generalization ability and, in some cases, introduce demographic biases that may have significant discriminative consequences when applied in real-life scenarios. By utilizing a more diverse multi-training dataset, we aim to mitigate these issues and create a more robust and fair deepfake detection system.

3.2 FSFM initialization

Among the recently available face foundation models, we selected FSFM [54] as our initialization point, owing to its strong generalization performance on face-related security tasks. While other approaches have aimed to learn general-purpose facial representations for downstream applications such as expression and attribute recognition, they primarily focus on salient facial features, that can be mimicked effectively by both spoofed and forged faces [65]. As a

result, these models often overlook the deeper authentic characteristics that are critical for face security tasks, and thus have limited applicability in such scenarios.

In contrast, FSFM is specifically designed to capture the intrinsic properties of real face images using a self-supervised learning (SSL) approach. It introduces a dual-branch pretraining framework that simultaneously leverages two complementary tasks: masked image modeling (MIM) and instance discrimination (ID). Each task is handled by a separate network branch, and the model is jointly optimized using three distinct objectives. It was pretrained on the VGGFace2 dataset [6], which contains approximately 3.3 million face images, providing a diverse and extended corpus for learning robust facial features.

After pretraining, the encoder $\mathcal{E}$ from the MIM branch, originally responsible for reconstructing masked regions during training, has learned rich, intrinsic representations of real faces and can be regarded as a face foundation model. We use this pretrained encoder to initialize our detector and we are extending it with a fully-connected classification layer to enable end-to-end fine-tuning.

3.3 Training objectives

The most commonly used loss in the deepfake detection domain is the binary softmax cross entropy loss. Given a mini-batch of B samples with class index labels $y_i \in \{0, 1\}$, the softmax cross-entropy loss is given by:

$$\mathcal{L}_{\text{BCE}} = -\frac{1}{B}\sum_{i=1}^{B}\log\left(\frac{e^{z_{i,y_i}}}{e^{z_{i,0}} + e^{z_{i,1}}}\right), \quad i \in [0, B),$$

where $\mathbf{z}$ are the classification logits.

Given its effectiveness in producing discriminative embeddings (Section 2.3), we employ an additional triplet loss [47] on the embeddings $H \in R^D$ generated by the encoder $\mathcal{E}$. Its main goal is to ensure that samples from the same class have embeddings that are closer to each other than to embeddings from different classes, thus enabling the classifier to better distinguish between real and fake samples. To achieve this, the triplet loss operates on triplets of samples (a, p, n), where a is the anchor, p is a positive sample (same class as the anchor), and n is a negative sample (different class). The objective is to bring the anchor and positive closer together in the embedding space while pushing the anchor and negative further apart. The triplet loss for a single triplet is defined as:

$$\mathcal{L}_{\text{tri}}(a, p, n) = \max\left(D_{a,p} - D_{a,n} + m,\ 0\right),$$

where $D_{i,j}$ denotes the Euclidean distance between the embeddings H_i and H_j, and m is a margin that enforces a minimum separation between positive and negative pairs. The overall training objective is defined as:

$$\mathcal{L} = \mathcal{L}_{\text{BCE}} + w \cdot \mathcal{L}_{\text{tri}},$$

where w is a weighting factor that controls the contribution of the triplet loss to the total objective.

3.3.1 Triplet mining. Based on the triplet loss definition, there are three categories of triplets (see Fig. 2):

- Easy triplets, where the negative is sufficiently far from the anchor, resulting in zero loss.
- Hard triplets, where the negative is closer to the anchor than the positive.

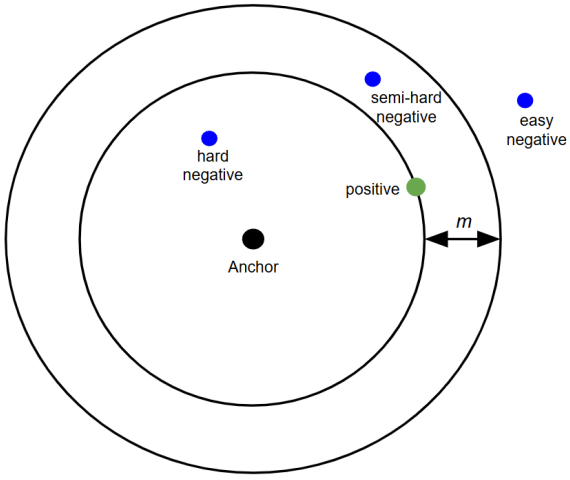

Figure 2: Depiction of easy, semi-hard and hard triplets.

- Semi-hard triplets, where the negative lies between the positive and the margin boundary.

All of the above definitions depend on the relative position of the negative sample with respect to the anchor and the positive. It is evident that easy triplets do not contribute to the optimization process, while hard and semi-hard triplets are the ones that actively influence it.

A critical aspect of triplet loss is the selection of triplets that are used in the loss computation. In our approach, we adopt an online mining strategy [47], where triplets are constructed dynamically within each training batch. This is much more efficient than offline mining, which involves forming triplets from the entire training set. Given a batch of size B, the set of valid triplets is defined as:

$$\mathcal{V} = \left\{(i, j, k) \;\middle|\; y_i = y_j,\ y_i \neq y_k,\ i \neq j\right\},$$

where $i, j, k \in [0, B)$ are batch indices corresponding to the anchor, positive, and negative samples, respectively. Once the embeddings for the samples are obtained, we must determine which of the valid triplets will be used for loss computation. Here we follow three different strategies:

Batch All (BA). This strategy considers all valid triplets within a batch and averages the loss over only the *active* triplets—i.e., those that are hard or semi-hard—while ignoring easy triplets that yield zero loss. Although similar approaches had been explored earlier [11, 53], Hermans et al. [20] were the first to highlight the importance of averaging only over the active subset. As training progresses and previously hard or semi-hard triplets become easy, they are excluded from the loss computation. This ensures that the training process continues to focus on the most informative triplets that still violate the margin and require adjustment. The BA triplet loss is given by:

$$\mathcal{L}_{\text{BA}} = \frac{1}{|\mathcal{V}_+|}\sum_{(i,j,k)\in\mathcal{V}_+}\left[D_{i,j} - D_{j,k} + m\right],$$

where $\mathcal{V}_+$ is the set of active triplets.

Hard Positive – Hard Negative (HP-HN). For each anchor sample in the batch, this strategy selects the *hardest positive* (i.e., the most distant positive sample) and the *hardest negative* (i.e., the closest negative sample). These triplets are considered the most informative, as they contribute most significantly to the loss [20]. By forcing the model to learn from the most challenging examples, this approach aims to improve generalization, potentially enabling the network to handle easier cases more effectively. However, such hard mining strategies have been reported to cause instability during the early stages of training, particularly when the selected triplets are too difficult [47]. The HP-HN triplet loss is given by:

$$\mathcal{L}_{\text{HP-HN}} = \frac{1}{B}\sum_{i=1}^{B}\left[\max\left(D_{i,HP_i} - D_{i,HN_i} + m,\ 0\right)\right],$$

where HP_i and HN_i are the hard positives and hard negatives of the anchor i, respectively.

Easy Positive – Hard Negative (EP-HN). For each anchor sample in the batch, this strategy selects the *easiest positive* (i.e., the closest positive sample) and the *hardest negative* (i.e., the closest negative sample). The idea of "easy positive mining" was first explored by Xuan et al. [59] as a means to mitigate over-clustering in the embedding space. This issue is particularly common in tasks involving large classes with high intra-class variance, where hard mining often selects positives that are so dissimilar to the anchor that pulling them close becomes infeasible. In contrast, easy positive mining has been shown to encourage the formation of more flexible embeddings that generalize better to unseen data [59]. The EP-HN triplet loss is given by:

$$\mathcal{L}_{\text{EP-HN}} = \frac{1}{B}\sum_{i=1}^{B}\left[\max\left(D_{i,EP_i} - D_{i,HN_i} + m,\ 0\right)\right],$$

where EP_i and HN_i are the easy positives and hard negatives of the anchor i, respectively.

3.4 Attribution

Deepfake detection is usually formulated as a binary classification problem, treating all manipulated content as belonging to a single "fake" class. However, in multi-source training datasets, such as the one used in our study, deepfake samples usually exhibit high diversity. This variation can be attributed to two main factors.

The first is the type of deepfake manipulation. Different manipulation techniques produce distinct visual artifacts and affect different facial regions. For example, face swapping methods replace the entire face, while face reenactment techniques modify only a subset of the facial features. These manipulation types also rely on fundamentally different generation techniques.

The second factor relates to the origin of each deepfake dataset. Each dataset employs its own manipulation methods and is built based on source videos captured in specific filming conditions, which may differ significantly from those in other datasets. These differences can further enhance the intra-class variability within the "fake" class.

We hypothesize that encouraging the model to differentiate between various types of deepfakes during training can lead to a more structured and semantically separated embedding space, thereby improving generalization performance. Motivated by this, we experiment with an attribution-based training approach, where the goal is not only to distinguish real from fake videos but also to assign distinct labels to different categories of deepfakes encountered during training. Specifically, we explore two attribution strategies:

- **Attribution by category ($\text{Att}_{\text{categ}}$).** In this setting, we distinguish between the two major deepfake categories: face swapping (FS) and face reenactments (RE). This reformulates the task into a three-class classification problem: one class for real videos and two separate classes for deepfakes, namely FS and RE.
- **Attribution by dataset ($\text{Att}_{\text{dataset}}$).** Here, we assign a separate label to deepfakes from each of the five datasets used in our training set. The resulting classification task involves one real class and five fake classes—one for each dataset.

At inference time, models trained with attribution are still used as binary classifiers by adding the probabilities of all fake attribution classes into a single universal "fake" class.

4 Experimental Setup

4.1 Training data

As reported in Section 3.1, our models were trained on an ensemble of deepfake datasets aiming to increase their real-world detection performance. To this end, we compiled an aggregated dataset combining the five previously mentioned deepfake datasets: FaceForensics (FF++) [46], Celeb-DF [33], DFDC [12], FakeAVCeleb [25] and ForgeryNet [19]. As shown in Table 1, the new dataset covers a wide range of both FS and RE manipulations (24 in total), with FS being the majority. During training, we employed the training and validation splits of the new aggregated dataset, which were compiled from the original splits, and consists of more than 226,000 videos.

Data pre-processing. All videos were sampled at 1 FPS rate and the RetinaFace [10] face detector was applied on the sampled frames. The bounding boxes of detected faces were enlarged by a margin of 30%, and after being cropped, were resized to 224x224.

Dataset sampling. Due to the significant class imbalance (Table 1) and the presence of a large number of highly similar samples, we employed a sampling strategy to construct a balanced training dataset with an approximately 1:1 real-to-fake ratio. To ensure diversity and representation, we enforced equal sampling across videos, guaranteeing that at least one sample from each video was included. The resulting training dataset comprised approximately 304K real and 287K fake samples. We also conducted experiments using the full set of samples, but they did not yield performance improvements and instead led to considerably longer training times.

4.2 Evaluation data

Our evaluation scheme is structured around three complementary directions: in-distribution, out-of-distribution, and in-the-wild evaluation. Each of them is designed to assess different aspects of the model's performance and generalization capabilities.

In-distribution testing. We first evaluate the performance of our models on the test sets of the five employed datasets. This evaluation reflects how well the models perform on manipulation

Table 1: Statistics of the training datasets used in our study. Training samples correspond to cropped faces from sampled video frames.

	Manipulations		Videos per split			Videos per class		Training samples	
	FS	RE	Train	Val	Test	Real	Fake	Real	Fake
FF++	3	2	4,320	840	840	1000	5000	12K	14K
Celeb-DF	1	-	6,010	-	518	889	5,639	9K	10K
DFDC	7	-	119,154	4,000	5,000	23,654	104,500	198K	194K
FakeAVCeleb	2	1	14,720	3,149	3,172	498	20,543	3K	14K
ForgeryNet	5	3	64,197	9,982	13,522	48,164	39,537	82K	55K
Total	18	6	208,401	17,971	23,052	74,205	175,219	304K	287K

Table 2: Number of videos (frames) for the "in-the-wild" datasets used in our evaluation.

	Real	Fake	Total
WDF	3,805 (46K)	3,509 (76K)	7,314 (122K)
ITW	402 (60K)	338 (24K)	740 (84K)
DF-Eval-2024	112 (14K)	964 (58K)	1,076 (72K)

types and settings seen during training, as these samples originate from the same distribution. The number of test videos per dataset is shown in Table 1. It is worth noting that we exclude from the FakeAVCeleb evaluation any samples labeled as "Real Video – Fake Audio", since our approach does not process the audio modality.

Out-of-distribution testing. Secondly, we assess the models' ability to generalize to a broader set of deepfake manipulations not seen during training. For this purpose, we conducted experiments on the recently released DF40 dataset [61]. DF40 includes some of the most advanced and up-to-date deepfake generation methods, spanning from 2019 to 2023. For our assessment, we used its test set, which contains 11,544 videos (178 real and 11,366 deepfakes). These were created by applying 9 face swapping (FS) and 12 reenactment (RE) techniques on real videos of the Celeb-DF test set.

In-the-wild testing. Finally, we evaluate our models on datasets with real-world cases that were collected from publicly available online content (Table 2). These in-the-wild datasets feature manipulations of unknown origin and diverse filming conditions, effectively simulating realistic application scenarios. To this end, we utilized the following three datasets. The first is the WDF dataset [67], released in 2020, which comprises 7,314 face sequences (3,805 real and 3,509 deepfakes) extracted from 707 videos collected from online sources. The second dataset, referred to as ITW, is an internal in-the-wild collection that we have been curating over the past five years with the help of professional fact checkers. It consists of 740 videos, including 402 pristine and 338 manipulated samples, all sourced from publicly available online content. Indicative statistics of the dataset can be found in Fig. 3. Lastly, we employ the Deepfake-Eval-2024 dataset [7], which contains recent deepfakes gathered from social media platforms and user submissions to deepfake detection systems throughout 2024. Although this dataset includes annotations for both video and audio modalities, we focused solely on the visual annotations and removed samples labeled as 'Unknown'. The resulting subset consists of 1,076 videos (112 real and 964 deepfakes).

The combination of these three in-the-wild datasets, each representing a distinct temporal window, offers a robust and diverse benchmark for evaluating the real-world generalization capabilities of our models. To ensure consistency, we applied to videos from ITW and Deepfake-Eval-2024 the same preprocessing pipeline as in training. For WDF, where only face sequences are available and not videos, we sampled every 10th face.

4.3 Models and Implementation

All our models share the same architecture (ViT-Base-16 [13]) and were trained on the same dataset. For the FSFM-based configurations, we initialized the models with the pretrained weights released by Wang et al. [54]. A fully connected layer was added on top of the encoder, following the average pooling of all non-CLS token features. These pooled features form the embeddings that are used for the triplet loss computation and their dimensionality is $D = 768$.

We explored three variants of the triplet loss discussed in Section 3.3: Batch All (BA), Hard Positive–Hard Negative (HP-HN), and Easy Positive–Hard Negative (EP-HN). The weighting factor w and *margin* hyperparameters were selected via empirical tuning, with the reported models corresponding to the best-performing configurations. In particular, w was chosen such that the BCE and triplet loss components contributed comparably, each operating within a similar value range, ensuring balanced optimization.

For the attribution experiments, we considered the two variants presented in Section 3.4: one that groups samples by manipulation category ($\text{Att}_{\text{categ}}$) and another that groups them by dataset source ($\text{Att}_{\text{dataset}}$).

All models were trained for 30 epochs with a batch size of 64, and the checkpoint with the lowest validation loss was retained. Optimization was performed using AdamW [40] with a weight decay of 0.05. Layer-wise learning rate decay was applied with a decay factor of 0.75 and a basic learning rate of 0.0001. We adopted also a cosine decay [39] learning rate schedule with linear warm-up over the first 5 epochs. Finally, we employed the same data augmentation strategy as in [54].

For comparison, we also conducted experiments with SBI [48], a prominent frame-based method that uses pseudo-negatives during training to improve generalization. As evaluation metrics, we employed the ROC-AUC and the balanced accuracy (bACC) with

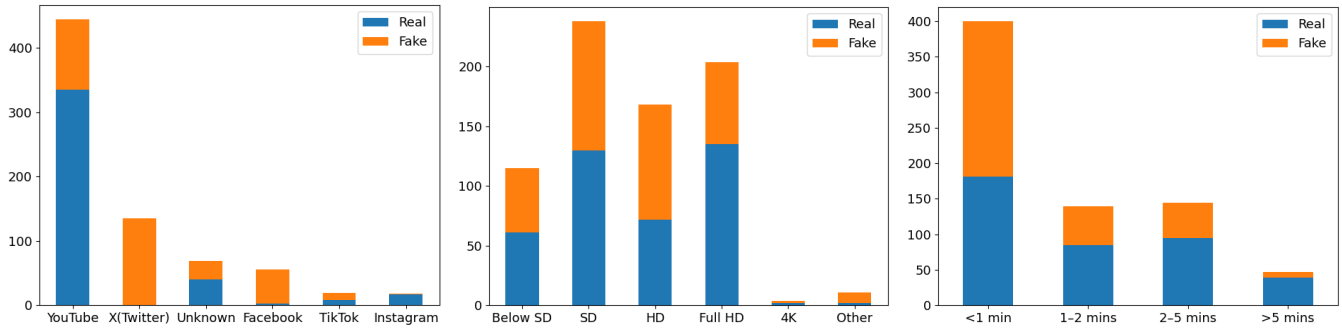

(a) Videos source **(b) Videos resolution** **(c) Videos duration**

Figure 3: Label-wise statistics of the ITW dataset.

0.5 threshold. Both metrics were computed at the video level by averaging the model predictions for all faces in a video.

5 Results and Discussion

The evaluation results across the three test scenarios for both metrics are presented in Table 3. For the in-distribution and in-the-wild scenarios, the average results across datasets are also reported. In the out-of-distribution scenario, we report the averaged metrics across all face swapping (FS), reenactment (RE), and total manipulation methods of the DF40 dataset.

5.1 Impact of FSFM

We first investigate the impact of using a face foundation model as the initialization point for training, compared to the conventional approach of using an ImageNet-pretrained backbone. When evaluated on the training data distribution, the ImageNet-pretrained model achieves a higher average bACC score, largely due to superior performance on the FF++ and FakeAVCeleb datasets. In contrast, the FSFM-initialized model shows a clear advantage only on the ForgeryNet dataset.

However, the benefits of the face foundation model become evident in the other two more challenging scenarios. On the DF40 dataset (out-of-distribution), FSFM leads to significant improvements in both AUC and bACC, by 7.6% and 11.1% respectively, with notable gains across both FS and RE categories. Similarly, in-the-wild testing shows consistent improvements across all three datasets, with average increases of approximately 3-4% in both metrics.

These results demonstrate that initializing with a face foundation model can substantially enhance the generalization performance of deepfake detection systems. Notably, the competing SBI method clearly underperforms across most of the scenarios compared to both the ImageNet- and FSFM-pretrained models, highlighting the effectiveness of our multi-dataset training strategy.

5.2 Impact of Triplet loss

Here, we examine the impact of incorporating the triplet loss into training, comparing the three variants that were presented in Section 3.3 against the standard binary cross-entropy (BCE) setup. In the in-distribution setting, AUC scores remain largely unchanged across most datasets, with the exception of ForgeryNet, where the HP-HN variant provides a modest 1% improvement. However, with respect to the bACC metric, we observe a drop in average performance, particularly with the HP-HN loss.

In the out-of-distribution scenario, the BA variant consistently outperforms the FSFM baseline, yielding an average increase of 0.6% in AUC and 1.7% in bACC. In contrast, the HP-HN variant clearly underperforms and fails to generalize well, achieving the lowest scores among all comparing variants and the baseline.

Under real-world settings, BA again emerges as the most robust variant. It achieves the highest overall average AUC and bACC, performing especially well on the ITW dataset. On the other hand, HP-HN and EP-HN perform comparable to the FSFM baseline. Notably, all three variants struggle the most on the WDF dataset. Overall, among the three triplet-loss configurations, the BA variant consistently delivers the best performance across all evaluation scenarios, surpassing the FSFM baseline, whereas HP-HN and EP-HN offer only limited or inconsistent benefits.

5.3 Impact of Attribution

Here, we evaluate the impact of training on multiple attribution labels instead of the standard binary classification, based on the two variants described in Section 3.4. In the in-distribution setting, the $\text{Att}_{\text{categ}}$ variant yields a modest improvement of 0.5% in AUC and 1.7% in bACC compared to the binary FSFM-initialized baseline, achieving the highest overall performance in this scenario. In contrast, the $\text{Att}_{\text{dataset}}$ variant shows less consistent results by offering a higher bACC but a lower AUC. The addition of the BA triplet loss slightly improves both variants in terms of AUC, but leads to a decline in bACC.

In the out-of-distribution evaluation on DF40, the $\text{Att}_{\text{categ}}$ variant underperforms, falling below the baseline on both metrics, mainly due to weaker results on RE manipulations. On the other hand, the $\text{Att}_{\text{dataset}}$ variant remains inconsistent. While it achieves the highest overall AUC, especially due to strong RE performance, its bACC is notably lower than all competing methods. This discrepancy suggests poor model calibration around the 0.5 decision threshold. Incorporating the triplet loss into both configurations generally leads to improved performance, with the exception of the $\text{Att}_{\text{dataset}}$ variant in terms of AUC, where a substantial drop is observed.

Table 3: Evaluation results in terms of video-level AUC and Balanced Accuracy across all three testing scenarios: in-distribution, out-of-distribution, and in-the-wild. For each scenario, the average results across datasets are also displayed. In the out-of-distribution case, the displayed metrics are averaged across different manipulation methods.

		In-distribution						Out-of-distribution			In-the-wild			
		FF++	CDF	DFDC	FakeAV	FNet	**Avg**	FS_{avg}	RE_{avg}	**Avg**	WDF	ITW	DF-Eval	**Avg**
AUC (%)	SBI [48]	88.2	91.0	73.4	99.3	64.2	83.2	82.8	56.3	67.6	74.8	68.0	54.4	65.7
	ImageNet pretrained	**99.3**	**100**	97.3	**100**	85.9	96.5	88.1	70.4	78.0	91.3	76.6	54.3	74.0
	FSFM	96.0	99.8	**97.8**	99.5	88.8	96.4	95.0	78.6	85.6	**93.1**	82.8	57.4	77.7
	FSFM + BA	96.9	99.9	97.0	99.6	89.5	96.6	95.3	**79.4**	86.2	92.7	**83.7**	57.4	**77.9**
	FSFM + HP-HN	95.7	99.8	97.5	99.4	**89.8**	96.4	94.3	77.2	84.5	92.0	83.1	**57.5**	77.5
	FSFM + EP-HN	96.8	99.8	96.9	99.5	88.9	96.4	95.3	78.8	85.9	92.8	83.1	56.6	77.5
	FSFM + Att_{categ}	98.4	**100**	97.1	99.9	88.7	96.8	95.6	76.4	84.6	91.5	80.2	55.9	75.9
	FSFM + Att_{categ} + BA	97.9	**100**	97.2	99.9	89.5	**96.9**	**95.8**	77.8	85.5	91.4	81.1	**57.5**	76.7
	FSFM + $Att_{dataset}$	97.9	**100**	97.3	**100**	85.8	96.0	95.6	**79.4**	**86.3**	91.9	79.6	55.8	75.8
	FSFM + $Att_{dataset}$ + BA	97.5	**100**	97.6	99.9	87.3	96.5	94.5	77.4	84.7	92.3	79.4	56.8	76.2
Balanced Accuracy (%)	SBI [48]	70.0	81.3	58.8	87.4	57.2	70.9	75.3	53.7	63.0	67.2	54.9	52.3	58.1
	ImageNet pretrained	**97.1**	97.2	91.5	**99.2**	77.8	**92.5**	70.6	54.7	61.5	83.7	63.9	55.5	67.7
	FSFM	90.3	97.6	**92.6**	92.4	81.3	90.8	83.7	64.3	72.6	**85.3**	72.4	55.6	71.2
	FSFM + BA	92.3	98.2	91.0	89.4	81.4	90.5	85.3	**66.1**	**74.3**	83.7	**74.8**	57.3	**71.9**
	FSFM + HP-HN	92.0	97.3	91.4	87.2	81.3	89.8	84.1	64.4	72.9	82.6	72.5	**57.4**	70.8
	FSFM + EP-HN	92.4	96.7	91.4	90.8	81.1	90.5	84.6	64.6	73.2	84.4	72.5	57.3	71.4
	FSFM + Att_{categ}	95.5	99.2	91.2	95.4	80.9	**92.5**	84.3	62.1	71.6	83.0	70.3	55.3	69.6
	FSFM + Att_{categ} + BA	94.7	99.2	91.1	92.5	**81.6**	91.8	**85.5**	63.5	73.0	83.3	71.6	56.3	70.4
	FSFM + $Att_{dataset}$	93.4	**99.6**	92.4	98.5	77.7	92.3	76.6	56.4	65.1	83.9	68.1	55.1	69.0
	FSFM + $Att_{dataset}$ + BA	93.5	**99.6**	92.3	95.5	78.7	91.9	77.4	58.3	66.5	84.5	68.1	56.6	69.7

Under in-the-wild testing, both attribution variants perform comparably but result in a noticeable decline in overall performance. Although the addition of the BA triplet loss yields minor improvements across all datasets and settings, these gains are not sufficient to match or surpass the FSFM-pretrained baseline.

In conclusion, while in some cases the attribution variants show promising results either on in-distribution settings (Att_{categ}) or on out-of-distribution ones ($Att_{dataset}$), they struggle to generalize in real-world scenarios. Consistent with previous findings, the inclusion of the BA triplet loss generally contributes positively, but cannot fully compensate for the shortcomings of the attribute variants under unknown conditions.

6 Conclusion

In this work, we explored several strategies to enhance the generalization capabilities of deepfake detectors in real-world scenarios. First, we trained our model on a collection of deepfake datasets, capturing a wide range of manipulation types and capturing conditions. We also leveraged a state-of-the-art face foundation model, which can offer a strong initialization point for our experiments through its rich, self-supervised facial representations. Additionally, we examined the incorporation of different triplet loss variants to improve the discriminative power of the learned embeddings. Finally, we investigated attribution-based labeling strategies as an alternative to standard binary classification. Extensive experiments across three evaluation settings (in-distribution, out-of-distribution, in-the-wild) revealed that multi-dataset training and initialization with face foundation models substantially boost detection performance, while the addition of triplet loss, particularly the 'Batch All' variant, yields modest additional gains. On the other hand, attribution strategies struggled to generalize to in-the-wild cases.

Acknowledgments

This work was partially funded by the EU Horizon Europe projects AI-CODE (Grant Agreement No. 101135437) and vera.ai (Grant Agreement No. 101070093).

References

[1] Spiros Baxevanakis, Manos Schinas, and Symeon Papadopoulos. 2025. Do DeepFake Attribution Models Generalize? *arXiv preprint arXiv:2505.21520* (2025).

[2] Luca Bondi, Edoardo Daniele Cannas, Paolo Bestagini, and Stefano Tubaro. 2020. Training strategies and data augmentations in cnn-based deepfake video detection. In *2020 IEEE international workshop on information forensics and security (WIFS)*. IEEE, 1–6.

[3] Stella Bounareli, Christos Tzelepis, Vasileios Argyriou, Ioannis Patras, and Georgios Tzimiropoulos. 2023. Hyperreenact: one-shot reenactment via jointly learning to refine and retarget faces. In *Proceedings of the IEEE/CVF International Conference on Computer Vision*. 7149–7159.

[4] Adrian Bulat, Shiyang Cheng, Jing Yang, Andrew Garbett, Enrique Sanchez, and Georgios Tzimiropoulos. 2022. Pre-training strategies and datasets for facial representation learning. In *European Conference on Computer Vision*. Springer, 107–125.

[5] Zhixi Cai, Shreya Ghosh, Kalin Stefanov, Abhinav Dhall, Jianfei Cai, Hamid Rezatofighi, Reza Haffari, and Munawar Hayat. 2023. Marlin: Masked autoencoder for facial video representation learning. In *Proceedings of the IEEE/CVF conference on computer vision and pattern recognition*. 1493–1504.

[6] Qiong Cao, Li Shen, Weidi Xie, Omkar M Parkhi, and Andrew Zisserman. 2018. Vggface2: A dataset for recognising faces across pose and age. In *2018 13th IEEE*

international conference on automatic face & gesture recognition (FG 2018). IEEE, 67–74.

[7] Nuria Alina Chandra, Ryan Murtfeldt, Lin Qiu, Arnab Karmakar, Hannah Lee, Emmanuel Tanumihardja, Kevin Farhat, Ben Caffee, Sejin Paik, Changyeon Lee, et al. 2025. Deepfake-eval-2024: A multi-modal in-the-wild benchmark of deepfakes circulated in 2024. *arXiv preprint arXiv:2503.02857* (2025).

[8] Bobby Chesney and Danielle Citron. 2019. Deep fakes: A looming challenge for privacy, democracy, and national security. *Calif. L. Rev.* 107 (2019), 1753.

[9] Jiankang Deng, Jia Guo, Niannan Xue, and Stefanos Zafeiriou. 2019. Arcface: Additive angular margin loss for deep face recognition. In *Proceedings of the IEEE/CVF conference on computer vision and pattern recognition*. 4690–4699.

[10] Jiankang Deng, Jia Guo, Yuxiang Zhou, Jinke Yu, Irene Kotsia, and Stefanos Zafeiriou. 2019. Retinaface: Single-stage dense face localisation in the wild. *arXiv preprint arXiv:1905.00641* (2019).

[11] Shengyong Ding, Liang Lin, Guangrun Wang, and Hongyang Chao. 2015. Deep feature learning with relative distance comparison for person re-identification. *Pattern Recognition* 48, 10 (2015), 2993–3003.

[12] Brian Dolhansky, Joanna Bitton, Ben Pflaum, Jikuo Lu, Russ Howes, Menglin Wang, and Cristian Canton Ferrer. 2020. The deepfake detection challenge (dfdc) dataset. *arXiv preprint arXiv:2006.07397* (2020).

[13] Alexey Dosovitskiy, Lucas Beyer, Alexander Kolesnikov, Dirk Weissenborn, Xiaohua Zhai, Thomas Unterthiner, Mostafa Dehghani, Matthias Minderer, Georg Heigold, Sylvain Gelly, et al. 2020. An image is worth 16x16 words: Transformers for image recognition at scale. *arXiv preprint arXiv:2010.11929* (2020).

[14] Chao Feng, Ziyang Chen, and Andrew Owens. 2023. Self-supervised video forensics by audio-visual anomaly detection. In *proceedings of the IEEE/CVF conference on computer vision and pattern recognition*. 10491–10503.

[15] Zheng Gao and Ioannis Patras. 2024. Self-supervised facial representation learning with facial region awareness. In *Proceedings of the IEEE/CVF Conference on Computer Vision and Pattern Recognition*. 2081–2092.

[16] Michael Goebel, Lakshmanan Nataraj, Tejaswi Nanjundaswamy, Tajuddin Manhar Mohammed, Shivkumar Chandrasekaran, and BS Manjunath. 2020. Detection, attribution and localization of gan generated images. *arXiv preprint arXiv:2007.10466* (2020).

[17] Alexandros Haliassos, Rodrigo Mira, Stavros Petridis, and Maja Pantic. 2022. Leveraging real talking faces via self-supervision for robust forgery detection. In *Proceedings of the IEEE/CVF conference on computer vision and pattern recognition*. 14950–14962.

[18] Alexandros Haliassos, Konstantinos Vougioukas, Stavros Petridis, and Maja Pantic. 2021. Lips don't lie: A generalisable and robust approach to face forgery detection. In *Proceedings of the IEEE/CVF conference on computer vision and pattern recognition*. 5039–5049.

[19] Yinan He, Bei Gan, Siyu Chen, Yichun Zhou, Guojun Yin, Luchuan Song, Lu Sheng, Jing Shao, and Ziwei Liu. 2021. Forgerynet: A versatile benchmark for comprehensive forgery analysis. In *Proceedings of the IEEE/CVF conference on computer vision and pattern recognition*. 4360–4369.

[20] Alexander Hermans, Lucas Beyer, and Bastian Leibe. 2017. In defense of the triplet loss for person re-identification. *arXiv preprint arXiv:1703.07737* (2017).

[21] Anubhav Jain, Pavel Korshunov, and Sébastien Marcel. 2021. Improving generalization of deepfake detection by training for attribution. In *2021 IEEE 23rd International Workshop on Multimedia Signal Processing (MMSP)*. IEEE, 1–6.

[22] Shan Jia, Xin Li, and Siwei Lyu. 2022. Model attribution of face-swap deepfake videos. In *2022 IEEE International Conference on Image Processing (ICIP)*. IEEE, 2356–2360.

[23] Liming Jiang, Ren Li, Wayne Wu, Chen Qian, and Chen Change Loy. 2020. Deeperforensics-1.0: A large-scale dataset for real-world face forgery detection. In *Proceedings of the IEEE/CVF conference on computer vision and pattern recognition*. 2889–2898.

[24] Mahmut Kaya and Hasan Şakir Bilge. 2019. Deep metric learning: A survey. *Symmetry* 11, 9 (2019), 1066.

[25] Hasam Khalid, Shahroz Tariq, Minha Kim, and Simon S Woo. 2021. FakeAVCeleb: A novel audio-video multimodal deepfake dataset. *arXiv preprint arXiv:2108.05080* (2021).

[26] Brandon Khoo, Raphaël C-W Phan, and Chern-Hong Lim. 2022. Deepfake attribution: On the source identification of artificially generated images. *Wiley Interdisciplinary Reviews: Data Mining and Knowledge Discovery* 12, 3 (2022), e1438.

[27] Pavel Korshunov, Anubhav Jain, and Sébastien Marcel. 2022. Custom attribution loss for improving generalization and interpretability of deepfake detection. In *ICASSP 2022-2022 IEEE International Conference on Acoustics, Speech and Signal Processing (ICASSP)*. IEEE, 8972–8976.

[28] Christos Koutlis and Symeon Papadopoulos. 2024. DiMoDif: Discourse Modality-information Differentiation for Audio-visual Deepfake Detection and Localization. *arXiv preprint arXiv:2411.10193* (2024).

[29] Alex Krizhevsky, Ilya Sutskever, and Geoffrey E Hinton. 2012. Imagenet classification with deep convolutional neural networks. *Advances in neural information processing systems* 25 (2012).

[30] Akash Kumar, Arnav Bhavsar, and Rajesh Verma. 2020. Detecting deepfakes with metric learning. In *2020 8th international workshop on biometrics and forensics (IWBF)*. IEEE, 1–6.

[31] Chunyu Li, Chao Zhang, Weikai Xu, Jinghui Xie, Weiguo Feng, Bingyue Peng, and Weiwei Xing. 2024. LatentSync: Audio Conditioned Latent Diffusion Models for Lip Sync. *arXiv preprint arXiv:2412.09262* (2024).

[32] Lingzhi Li, Jianmin Bao, Hao Yang, Dong Chen, and Fang Wen. 2019. Faceshifter: Towards high fidelity and occlusion aware face swapping. *arXiv preprint arXiv:1912.13457* (2019).

[33] Yuezun Li, Xin Yang, Pu Sun, Honggang Qi, and Siwei Lyu. 2020. Celeb-df: A large-scale challenging dataset for deepfake forensics. In *Proceedings of the IEEE/CVF conference on computer vision and pattern recognition*. 3207–3216.

[34] Yuzhen Lin, Wentang Song, Bin Li, Yuezun Li, Jiangqun Ni, Han Chen, and Qiushi Li. 2024. Fake it till you make it: Curricular dynamic forgery augmentations towards general deepfake detection. In *European Conference on Computer Vision*. Springer, 104–122.

[35] Kunlin Liu, Ivan Perov, Daiheng Gao, Nikolay Chervoniy, Wenbo Zhou, and Weiming Zhang. 2023. Deepfacelab: Integrated, flexible and extensible face-swapping framework. *Pattern Recognition* 141 (2023), 109628.

[36] Yu Liu, Hongyang Li, and Xiaogang Wang. 2017. Rethinking feature discrimination and polymerization for large-scale recognition. *arXiv preprint arXiv:1710.00870* (2017).

[37] Yuanyuan Liu, Wenbin Wang, Yibing Zhan, Shaoze Feng, Kejun Liu, and Zhe Chen. 2023. Pose-disentangled contrastive learning for self-supervised facial representation. In *Proceedings of the IEEE/CVF conference on computer vision and pattern recognition*. 9717–9728.

[38] Yu-Cheng Liu, Chia-Ming Chang, I-Hsuan Chen, Yu-Ru Ku, and Jun-Cheng Chen. 2021. An experimental evaluation of recent face recognition losses for deepfake detection. In *2020 25th International Conference on Pattern Recognition (ICPR)*. IEEE, 9827–9834.

[39] Ilya Loshchilov and Frank Hutter. 2016. Sgdr: Stochastic gradient descent with warm restarts. *arXiv preprint arXiv:1608.03983* (2016).

[40] Ilya Loshchilov and Frank Hutter. 2017. Decoupled weight decay regularization. *arXiv preprint arXiv:1711.05101* (2017).

[41] Dat Nguyen, Nesryne Mejri, Inder Pal Singh, Polina Kuleshova, Marcella Astrid, Anis Kacem, Enjie Ghorbel, and Djamila Aouada. 2024. Laa-net: Localized artifact attention network for quality-agnostic and generalizable deepfake detection. In *Proceedings of the IEEE/CVF Conference on Computer Vision and Pattern Recognition*. 17395–17405.

[42] Yuval Nirkin, Yosi Keller, and Tal Hassner. 2019. Fsgan: Subject agnostic face swapping and reenactment. In *Proceedings of the IEEE/CVF international conference on computer vision*. 7184–7193.

[43] Trevine Oorloff, Surya Koppisetti, Nicolò Bonettini, Divyaraj Solanki, Ben Colman, Yaser Yacoob, Ali Shahriyari, and Gaurav Bharaj. 2024. Avff: Audio-visual feature fusion for video deepfake detection. In *Proceedings of the IEEE/CVF Conference on Computer Vision and Pattern Recognition*. 27102–27112.

[44] KR Prajwal, Rudrabha Mukhopadhyay, Vinay P Namboodiri, and CV Jawahar. 2020. A lip sync expert is all you need for speech to lip generation in the wild. In *Proceedings of the 28th ACM international conference on multimedia*. 484–492.

[45] Yuyang Qian, Guojun Yin, Lu Sheng, Zixuan Chen, and Jing Shao. 2020. Thinking in frequency: Face forgery detection by mining frequency-aware clues. In *European conference on computer vision*. Springer, 86–103.

[46] Andreas Rössler, Davide Cozzolino, Luisa Verdoliva, Christian Riess, Justus Thies, and Matthias Nießner. 2018. Faceforensics: A large-scale video dataset for forgery detection in human faces. *arXiv preprint arXiv:1803.09179* (2018).

[47] Florian Schroff, Dmitry Kalenichenko, and James Philbin. 2015. Facenet: A unified embedding for face recognition and clustering. In *Proceedings of the IEEE conference on computer vision and pattern recognition*. 815–823.

[48] Kaede Shiohara and Toshihiko Yamasaki. 2022. Detecting deepfakes with self-blended images. In *Proceedings of the IEEE/CVF conference on computer vision and pattern recognition*. 18720–18729.

[49] Aliaksandr Siarohin, Stéphane Lathuilière, Sergey Tulyakov, Elisa Ricci, and Nicu Sebe. 2019. First order motion model for image animation. *Advances in neural information processing systems* 32 (2019).

[50] Jiahe Tian, Cai Yu, Xi Wang, Peng Chen, Zihao Xiao, Jiao Dai, Jizhong Han, and Yesheng Chai. 2024. Real appearance modeling for more general deepfake detection. In *European Conference on Computer Vision*. Springer, 402–419.

[51] Ruben Tolosana, Ruben Vera-Rodriguez, Julian Fierrez, Aythami Morales, and Javier Ortega-Garcia. 2020. Deepfakes and beyond: A survey of face manipulation and fake detection. *Information Fusion* 64 (2020), 131–148.

[52] Ashish Vaswani, Noam Shazeer, Niki Parmar, Jakob Uszkoreit, Llion Jones, Aidan N Gomez, Łukasz Kaiser, and Illia Polosukhin. 2017. Attention is all you need. *Advances in neural information processing systems* 30 (2017).

[53] Faqiang Wang, Wangmeng Zuo, Liang Lin, David Zhang, and Lei Zhang. 2016. Joint learning of single-image and cross-image representations for person re-identification. In *Proceedings of the IEEE conference on computer vision and pattern recognition*. 1288–1296.

[54] Gaojian Wang, Feng Lin, Tong Wu, Zhenguang Liu, Zhongjie Ba, and Kui Ren. 2025. Fsfm: A generalizable face security foundation model via self-supervised facial representation learning. In *Proceedings of the Computer Vision and Pattern Recognition Conference*. 24364–24376.

[55] Jiadong Wang, Xinyuan Qian, Malu Zhang, Robby T Tan, and Haizhou Li. 2023. Seeing what you said: Talking face generation guided by a lip reading expert. In *Proceedings of the IEEE/CVF Conference on Computer Vision and Pattern Recognition*. 14653–14662.

[56] Yue Wang, Jinlong Peng, Jiangning Zhang, Ran Yi, Liang Liu, Yabiao Wang, and Chengjie Wang. 2023. Toward high quality facial representation learning. In *Proceedings of the 31st ACM International Conference on Multimedia*. 5048–5058.

[57] Yaohui Wang, Di Yang, Francois Bremond, and Antitza Dantcheva. 2022. Latent Image Animator: Learning to Animate Images via Latent Space Navigation. In *International Conference on Learning Representations*. https://openreview.net/forum?id=7r6kDq0mK_

[58] Zhendong Wang, Jianmin Bao, Wengang Zhou, Weilun Wang, and Houqiang Li. 2023. Altfreezing for more general video face forgery detection. In *Proceedings of the IEEE/CVF conference on computer vision and pattern recognition*. 4129–4138.

[59] Hong Xuan, Abby Stylianou, and Robert Pless. 2020. Improved embeddings with easy positive triplet mining. In *Proceedings of the IEEE/CVF Winter Conference on Applications of Computer Vision*. 2474–2482.

[60] Zhiyuan Yan, Yuhao Luo, Siwei Lyu, Qingshan Liu, and Baoyuan Wu. 2024. Transcending forgery specificity with latent space augmentation for generalizable deepfake detection. In *Proceedings of the IEEE/CVF Conference on Computer Vision and Pattern Recognition*. 8984–8994.

[61] Zhiyuan Yan, Taiping Yao, Shen Chen, Yandan Zhao, Xinghe Fu, Junwei Zhu, Donghao Luo, Chengjie Wang, Shouhong Ding, Yunsheng Wu, et al. 2024. Df40: Toward next-generation deepfake detection. *arXiv preprint arXiv:2406.13495* (2024).

[62] Zhiyuan Yan, Yong Zhang, Yanbo Fan, and Baoyuan Wu. 2023. Ucf: Uncovering common features for generalizable deepfake detection. In *Proceedings of the IEEE/CVF International Conference on Computer Vision*. 22412–22423.

[63] Baiwu Zhang, Jin Peng Zhou, Ilia Shumailov, and Nicolas Papernot. 2020. On attribution of deepfakes. *arXiv preprint arXiv:2008.09194* (2020).

[64] Yinglin Zheng, Jianmin Bao, Dong Chen, Ming Zeng, and Fang Wen. 2021. Exploring temporal coherence for more general video face forgery detection. In *Proceedings of the IEEE/CVF international conference on computer vision*. 15044–15054.

[65] Yinglin Zheng, Hao Yang, Ting Zhang, Jianmin Bao, Dongdong Chen, Yangyu Huang, Lu Yuan, Dong Chen, Ming Zeng, and Fang Wen. 2022. General facial representation learning in a visual-linguistic manner. In *Proceedings of the IEEE/CVF conference on computer vision and pattern recognition*. 18697–18709.

[66] Jiaran Zhou, Yuezun Li, Baoyuan Wu, Bin Li, Junyu Dong, et al. 2024. Freqblender: Enhancing deepfake detection by blending frequency knowledge. *Advances in Neural Information Processing Systems* 37 (2024), 44965–44988.

[67] Bojia Zi, Minghao Chang, Jingjing Chen, Xingjun Ma, and Yu-Gang Jiang. 2020. Wilddeepfake: A challenging real-world dataset for deepfake detection. In *Proceedings of the 28th ACM international conference on multimedia*. 2382–2390.